



## Seismic Reliability Analysis of a Hybrid Timber-Steel Frame with Reduced Beam Section

Ariya Eini<sup>1\*</sup>, Mehdi Banazadeh<sup>2</sup>

<sup>1</sup>PhD Student, Department of Civil Engineering, University of Victoria, BC, Canada

<sup>2</sup>Associate Professor, Department of Civil Engineering, Amirkabir University of Technology, Tehran, Iran

\*[ariyaeni@uvic.ca](mailto:ariyaeni@uvic.ca) (Corresponding Author)

### ABSTRACT

This paper presents seismic reliability evaluation of a hybrid timber-steel frame. The structural system consists of glued-laminated timber beams and columns with replaceable steel connections. The steel link utilizes reduced beam section serving as the main energy-dissipative element that provides the required ductility for seismic design. Considering uncertainties in structural properties and seismic actions is important in seismic performance assessment. To capture epistemic uncertainties, structural models were developed considering varying yield base shear coefficients, connection lengths, and seismic weights. The response data set was created by performing Incremental Dynamic Analysis under a set of 22 ground motions representing aleatory uncertainties. The data set was then used to develop probabilistic demand models through Bayesian regression analysis which incorporates statistical uncertainty. The second-order reliability method was utilized in Rt software to calculate the reliability index. The study investigates the effect of structural properties on the reliability index under different performance objectives, and shows that the presented seismic assessment procedure demonstrated the efficiency of the hybrid timber-steel system. The probability of failure was less than 0.6% for all structures at a seismic hazard of 2% probability of exceedance in 50 years. The fragility curves obtained from regression-based models provided an accurate estimate of the results derived from IDA. The results show that the ready-made models reduce the need for the time-consuming collection of a large number of observations. The study's findings provide valuable insights into the seismic performance-based design of the hybrid timber-steel frame.

Keywords: Hybrid steel-timber frame, Reliability analysis, Bayesian regression, Seismic safety, Incremental Dynamic Analysis

### INTRODUCTION

The use of mass-timber moment-resisting frames (MRF) in multi-story buildings offers numerous advantages, such as a high strength-to-weight ratio that reduces foundation demands and seismic forces. Mass-timber elements can be rapidly assembled on site, resulting in faster construction times. In addition to the costs benefits, timber is a renewable material that reduces the carbon footprint of structures [1].

Steel moment resisting frames (MRF) as a flexible lateral load resisting system have shown sufficient seismic performance in the past earthquakes. However, the brittle nature of timber limits the design of timber MRFs to rely solely on the energy dissipation capacity of connections. Conventional connections in mass-timber MRFs may not provide enough ductility, stiffness and resiliency to meet the new code requirements. The 2020 National Building Code of Canada (NBCC 2020) [2] introduced a significant increase in seismic hazard spectrum compared to its predecessor guidelines.

Development of new connections are necessary to facilitate the convenient repair of timber MRFs in the aftermath of an earthquake. Recent studies have proposed novel steel joints for mass-timber MRFs with excellent performance. Andreolli et al. [3] introduced a steel-timber joint for moment resisting systems consisting of a steel stub with an end-plate and steel rods. Specimens with an end-plate thickness of 8 mm and 10 mm showed a static ductility ratio of 6 without more than a 20% reduction of their resistance, which were identified as highly ductile connections. Komatsu et al. [4, 5] designed a beam-column

using 45° inclined and 90° self-tapping screws combined with steel side plates and a shear resisting steel dowel. A glulam semi-rigid connection with lags crews using slotted bolted connection was developed to overcome the brittle failure mode of the joint.

A viable solution to the lack of ductility of timber MRFs would be to install replaceable steel sections at the beams ends, resulting in enhanced resiliency. Gilberth and Gohlich [6] introduced a new hybrid timber-steel MRF system with reduced beam sections (RBS) as moment-resisting connections. The connection has the advantage of having a steel cross section specially designed to act as a structural fuse. This link is a replaceable reduced steel beam section (RBS) which is fastened to timber elements using self-tapping screws and end-plates. Reference is made to this particular system that uses glulam (glue-laminated) beams equipped with steel links and seems to ensure the elastic behavior of all other members up to the collapse point [6]. This design methodology provides the necessary flexibility to facilitate realignment and re-centering of the structure. This approach allows for significant ductility gain in heavy timber MRFs compared to frames with traditional dowel type connections or even with advanced fasteners [7]. Having the failure of the steel section to precede both intermediate timber members and steel-timber connections, required energy dissipation could develop in steel devices. A six-story MRF structure with RBS connection was studied in the current study.

### Reliability Analysis

Reliability analyses in the context of Performance-Based Design (PBD) allow structures to be designed to meet specific target performance objectives. Seismic reliability analysis considers sources of uncertainty such as loading, structural weight, material properties, and geometrical characteristics to provide a comprehensive safety assessment of a structure. Seismic reliability has been refined and adapted for design and evaluation of steel and reinforced concrete structures during recent decades, while the basis for design of timber structures, in terms of reliability, is falling significantly behind. Papadrakakis et al. [8] presented a straightforward procedure for the reliability-based sizing structural optimization of seismic performance of steel frames. Khatibinia et al. [9] performed seismic reliability analysis on existing RC structures, proposing a metamodel with weighted least squares and wavelet weighted least squares support vector machine. This method reduced the computational cost of the Monte-Carlo Simulation. Kia and Banazadeh [10] developed the first generation of the demand model of the low to mid-rise regular steel moment frames. Then, based on the proposed model, closed-form fragility analyses are performed. They proposed the Bayesian regression-based demand and collapse models to cut data analysis time [11].

The probability of failure in structural safety assessment is calculated by considering the probabilistic models of acting loads (demand) and resistance of a structural system (capacity). The reliability methods find the probability that a limit state is exceeded under specific service conditions [12]. In general, the reliability problem can be formulated by:

$$P_f = \phi(-\beta) = \int_{\Omega} f_x(X) dx_1 dx_2 \dots dx_n \quad (1)$$

Where  $P_f$  is the probability of failure,  $\beta$  is the reliability index and  $\Omega$  is the failure domain. The probability density function of standard normal distribution is denoted by  $\phi$ . In case of considering  $n$  random variables ( $x_i$ ) that represent uncertainty,  $f_x(X)$  is the joint probability density function of the vector  $X = \{x_1, x_2, \dots, x_n\}$ . The limit-state function is defined as  $g(X)$ , Therefore,  $g(X) = 0$  is an  $n$ -dimensional surface that divides the domain into the safety and failure region [12]. However, solving this integral is very time-consuming if not impractical, but also there is usually no closed-form expression for Eq. (1). First-order reliability method (FORM), second-order reliability method (SORM), sampling and response surface method have been proposed to solve the component reliability problem [12].

When performing structural reliability analysis, it is common to encounter studies that involve a large grid of points resulting from implementation of multiple random variables. The response surface method (RSM) facilitates carrying out reliability analysis by an approximation of response database. RSM uses a series of parameter combinations. Furthermore, it evaluates the model at multiple trial points, then acts as a proxy to the demand model [13]. In this study, a number of properties of the developed generic frames have been selected to be varied, including the following: the seismic weight, seismic intensity, length of the steel connection, and  $C_y$  which is the ratio of yield base shear to the building weight (yield base shear coefficient). The aforementioned method makes it possible to explore the relationship between explanatory variables and multiple response variables. Structural damage to the building under a set of ground motions was quantified by the overall maximum interstorey drift (MISD) which has been conventionally used as the engineering demand parameter for structures. Response surfaces were generated using the uncertainties stated before and used to predict the MISD statistics. Then, the SORM analyses was performed to calculate the structural system reliability.

The aim is to assess the safety of this newly proposed assembly through reliability analysis considering uncertainties in input variables. The results of this study will provide valuable insights into quantifying ductility-related seismic force modification

factors of this hybrid steel-timber MRF. Hybrid MRF timber structures are usually designed based on conservative assumptions since there are no clear design guidelines on the timber MRF systems with highly ductile connections in NBCC [2]. The primary objective of this study was to utilize the response surface method and the Bayesian regression analysis for the probabilistic assessment of this hybrid steel-timber frame to save computation time for generation of seismic fragility curves.

## HYBRID STEEL-TIMBER FRAME

### Seismic Design and Numerical Models

A new hybrid steel-timber moment-resisting frame has been introduced by Gohlich [14]. It utilizes a reduced steel beam section (RBS) at the glulam beam-column joints, which potentially leads to a higher ductility level of the MRF systems with glulam columns and beams. Twenty-seven two-dimensional MRF structures were developed in this study. These models were designed to have a seven-bay frame. The structure layouts were similar to the preceding study [6], each bay spacing is 6.5 meters. All models are office buildings and have six stories, and each story is 3.7 m high. Glulam members made using Douglas Fir-Larch with a stress rating of 24f-EX [15].

Ductility-related force modification factors ( $R_d$ ) are essential to forced-based design of structures. The value of  $R_d = 2$  is assigned to timber MRFs with ductile connections and  $R_d = 5$  corresponds to ductile steel MRFs in NBCC [2]. To examine if a higher  $R_d$  could be considered safe for the design of the new hybrid steel-timber MRF, three reference models were designed with  $R_d = 2$ ,  $R_d = 3.5$ , and  $R_d = 5$ . These structures had fundamental periods of 2.05 s, 2.44 s and 2.85 s, respectively. The overstrength-related force modification factor ( $R_o$ ) was considered 1.5 as stated in NBCC. The initial calculated seismic weight was  $W = 19600$  kN. According to NBCC [2], the design period of six-storey timber frames is 0.6 s ( $T_a = 0.1N$ , where N is the number of storeys). The upper limit which is 1.5 times the empirical period, 0.9 seconds, was applied to obtain the spectral acceleration in the uniform hazard spectrum for Vancouver City Hall and site class C. The design spectral acceleration was  $S_{mt} = 0.58g$  for all structural models. Forces at the beam-column interface were used to design the links according to CISC [16]. The length ( $L$ ) of the reduced beam section was obtained for each of the reference cases. Then the capacity designed forces were calculated and used in the design of timber members according to CSA-O86 [15]. This procedure would ensure that the steel link yields and the nonlinear behavior is localized into the plastic hinge. Once the length of steel links was obtained, additional models with varying RBS lengths were developed which will be explained in the next section.

A leaning column was provided to account for p-delta effects. The periods of the nonlinear models were calculated 1.91, 2.3, and 2.63 for the structures designed with a  $R_d$  of 2, 3.5, and 5 respectively. These results verify the accuracy of modeling as the periods are close for both the nonlinear system in OpenSees [17] and the linear models. Prior to simulating the frames, a model representing the test specimen previously tested by Gohlich [14] was created to calibrate the behavior of each material and element. The beam-column joint of the test specimen model incorporated four main components: wood beams and columns, steel panel zone, gross steel link sections, and reduced steel link sections.

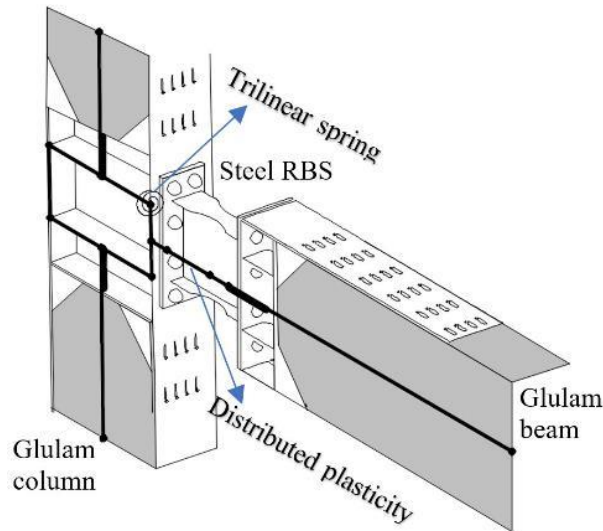


Figure 1. Timber-steel moment-resisting Connection [6] and OpenSees elements.

The glulam beam and column members were modeled using elastic beam-column elements as the wood is supposed to remain elastic. The RBS was modeled using three different elements. Since the tests showed that the plastic hinge occurred in the

middle of the link, an elastic element was located at both ends of the steel section. A distributed plasticity model with a displacement-based beam-column element was assigned to the middle dogbone section. The uniaxial Giuffre-Menegotto Pinto material [18] in OpenSees was assigned to fiber sections along RBS with five integration points. The steel panel zone was modeled with rigid elements, and its plastic behavior was presented as a trilinear rotational spring [19] as shown in Figure 1.

### Sources of Uncertainty

Ground motion-induced structural response uncertainty is an aleatory uncertainty which cannot be reduced by the modeler. Record-to-record variability and its uncertainty propagation at different seismic hazard levels are represented by scaling a suite of 44 far-field single records recommended by FEMA P-695 [20]. To widen the generality of the obtained demand models, a number of parameters of the hybrid frames have been selected to vary which takes into account the epistemic uncertainties. Three levels of seismic weight proportional to the initial calculated weight ( $W$ ), twenty levels of ground motion intensity proportional to the design uniform hazard spectrum ( $S_{mi}$ ), three levels of the RBS section length proportional to the mean value ( $L$ ) of the allowable range identified by CISC [16], and the calculated yield base shear coefficient ( $C_y$ ) are the extent of variants. Table 1 lists the ranges of the random variables for generating the response surface database ( $L$  and  $W$  are the length of the RBS and weight of reference structures, respectively). A total of 27 (3 seismic weights  $\times$  3 RBS length  $\times$  3  $R_d$  factors) structures were developed based on the combination of defined variables.

Table 1. Random variables and their range.

Variable	Range					COV
$i (S_{mi})$	25%	50%	75%	... 475%	500%	0.24
$l$	0.9L		L	1.1L		0.05
$w$	0.75W		W	1.25W		0.1
$C_y$	Low		Moderate	High		0.1

$C_y$  is the ratio of yield base shear to the structure's weight and is obtained from static pushover analysis. Designing a structure with low  $R_d$  factor will result in a higher resistance against lateral loads. Therefore, the  $C_y$  factors of buildings designed with  $R_d = 2$ ,  $R_d = 3.5$ , and  $R_d = 5$  are identified as "High", "Moderate" and "Low", respectively. Table 2 presents  $C_y$  for reference models designed by  $R_d = 2$ ,  $R_d = 3.5$ , and  $R_d = 5$  with the initial value of seismic weight and RBS length.

Table 2.  $C_y$  ratio in three basic prototype models.

Model No	$R_d$	$C_y$
1	5	0.13
2	3.5	0.18
3	2	0.26

A range from  $0.65d$  to  $0.85d$  for designing the dogbone detail of RBS is indicated in CISC [16] where  $d$  is the depth of section. The middle value of this range ( $0.75d$ ) is deemed to be used by most of the designers, therefore, it was used for the primary design of the reference structures. It was assumed that 95 % of times the connection length would be values that are 10 percent larger or 10 percent lower than the mean value. Therefore, the length of the reduced section was assumed to follow a normal distribution with a coefficient of variation (COV) of 0.05 as listed in Table 1. The seismic weight and  $C_y$  were assumed to have a normal distribution with a COV of 0.1. The ground excitation intensity follows a lognormal distribution, with a mean value equal to the uniform hazard spectrum and a COV of 0.24 which was obtained from the Geological Survey of Canada [21].

### Incremental Dynamic Analysis

To generate the database needed for reliability analysis, incremental dynamic analysis (IDA) was performed [22]. IDA utilizes increasingly scaled levels of intensity measure (spectral acceleration) for a selected set of ground motion records. 44 ground motions of FEMA P695 [20] were scaled to the 2% probability of exceedance in 50-years seismic hazard level which is the design level earthquake in NBCC [2]. The scaling of spectral acceleration was carried out on a period range of from 0.2 to 2 times the fundamental period of the structures. The structural responses are then recorded at each intensity level and scaling

continues until structural collapse occurrence is detected. Models were subjected to 25%, 50%, 75%, ..., 475% and 500% (increment of 0.25%) of the design level intensity ( $S_{mt}$ ). This resulted in 15445 dynamic analyses and maximum interstorey drift (MISD) recordings.

Dynamic instability is a crucial signal for potential collapse, and it can be determined by detecting the point on the IDA curve where the tangent slope is equal to 20% of the elastic slope. [23]. Glulam members, despite their high strength and stiffness, are prone to brittle behavior, the point at which these members reach their capacity can serve as another potential collapse point. Moreover, dynamic analyses indicated a significant increase in drift values around 5% interstorey drift ratio. Gohlich [14] reported link failure and excessive out of plane buckling in the test specimens at 0.05 rad rotation of the connection. To establish this drift value as a damage-based rule for collapse, the total connection rotation was captured during dynamic analysis. This rotation was obtained by recording the midpoint displacement of the beam and columns connected to the RBS. The results are presented in Table 3 and demonstrates that upon reaching the maximum interstorey drift ratio (MISD) of 0.05, the difference between connection rotation and the corresponding interstorey drift diminishes. This proves that at a near-collapse state, the rotation of the RBS connection approximates the interstorey drift ratio.

Table 3. Total connection rotation and the corresponding interstorey drift throughout the time history analysis.

Maximum interstorey drift ratio	Connection rotation (rad)	Relative difference %
0.0050	0.0040	18.8
0.0110	0.0092	16.4
0.0150	0.0131	12.7
0.0201	0.0176	12
0.0248	0.0225	9.3
0.0302	0.0272	9.9
0.0353	0.0322	8.5
0.0400	0.0371	7.3
0.0449	0.0470	-4.7
0.0501	0.0531	-5.8

Due to the mentioned reasons, a 5% drift was defined as a collapse criterion. The collapse of structures happens when half of the records cause failure of the model and  $S_{ct}$  is the spectral acceleration where median collapse capacity is observed. The IDA curves for the reference models with the initial calculated seismic weight ( $W$ ), RBS lengths ( $L$ ), and designed with  $R_d = 5$  (model 1),  $R_d = 3.5$  (model 2) and  $R_d = 2$  (model 3) are shown in Figure 2. The collapse capacity ( $S_{ct}$ ) for structures designed with a  $R_d$  of 5, 3.5 and 2 are 1.27g, 1.48g, and 1.71g, respectively. According to the CCMC design guideline [24], since the structure designed with  $R_d = 5$  has a collapse capacity which is larger than the 200% of the uniform hazard spectrum ( $S_{ct} / S_{mt} = 1.27g / 0.58g = 2.19 > 2$ ), the  $R_d = 5$  is deemed acceptable for seismic design of the hybrid steel-timber system.

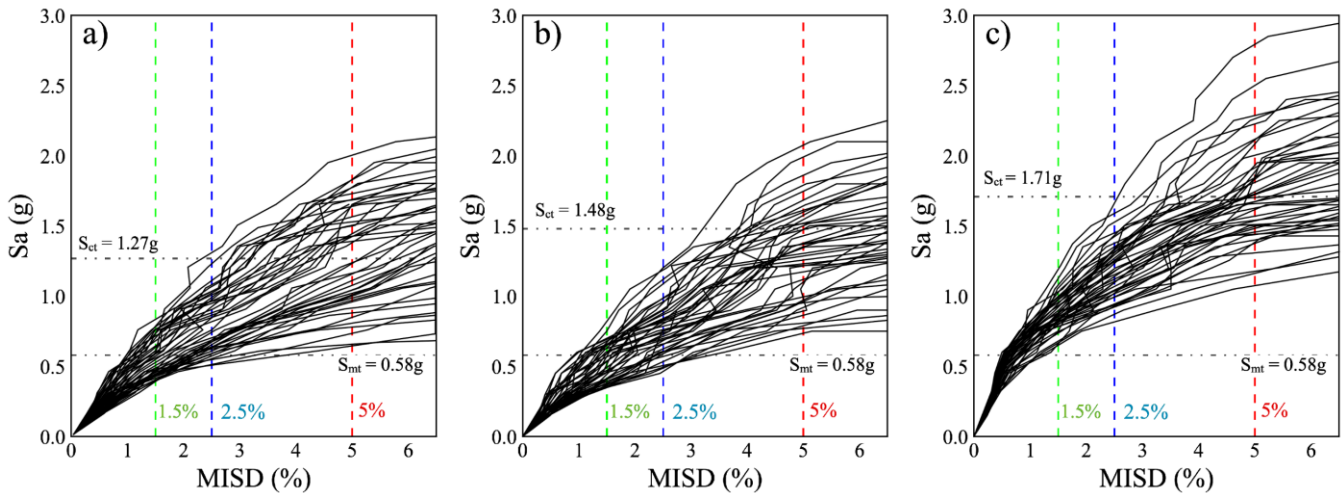


Figure 2. IDA curves of reference models: a) Model No.1; b) Model No.2; c) Model No.3.

## BAYESIAN REGRESSION INFERENCE

Performing reliability and probabilistic seismic demand analyses using the database generated by incremental dynamic analysis (IDA) can be a time-intensive task. To overcome this challenge, a mathematical algorithm incorporating a robust Bayesian approach has been utilized to perform curve-to-data best fit, streamlining the analysis process. The general linear regression model addressed in this paper has this form:

$$y = \theta_1 X_1 + \theta_2 X_2 + \dots + \theta_k X_k + \varepsilon \quad (2)$$

The response variable ( $y$ ) is predicted by the regression analysis.  $X$  denotes regressors formulated in terms of the explanatory variables, and  $\theta_i$  is the regression coefficient. In this study, the explanatory variables are seismic intensity ( $i$ ), RBS length ( $l$ ), seismic weight ( $w$ ) and yield base shear coefficient ( $C_y$ ). The function in Eq. (2) is considered as a linear regression because of the linear formulation with respect to  $\theta_i$ . Discrepancy between observations and predictions ( $\varepsilon$ ) is supposed to be a normal random variable. This method overcomes the shortcomings existing in the classical regression analysis and considers the statistical uncertainty by treating the regression coefficients and model error as random variables.

The mean and standard deviation of seismic demand (MISD) are needed as random variables in the definition of limit state function. In intensities beyond the design level earthquake, some seismic records result in structure collapse. Consequently, the number of non-collapsing interstorey drift values would be less than the total sample population (less than 44 records). In such cases, observations are restricted to a portion of the population values that are less than 0.05 (collapse drift value), resulting in truncated samples where some population values are entirely excluded. To overcome this problem, this study employed the maximum likelihood estimation of the probability density function's mean and variance. A lognormal model was developed at each intensity level to determine the distribution function of the seismic demand. The probability that a selected value of this database meets the requirements for inclusion in the sample that is singly truncated on the right at 0.05 was calculated. The relationship between the sample statistic and the population mean and standard deviation was investigated as formulated by Cohen [25]. This procedure improved the accuracy of the initial mean and standard deviation of non-collapsing records. The new values obtained from this method are more reliable than ignoring the effect of population reduction on the sample statistics.

From the response database, the mean,  $D_\mu$ , and standard deviation,  $D_\sigma$ , of the maximum interstorey drift were estimated through the Bayesian statistical inference with the use of polynomial functions. The absolute square error metric was used as a fitness function to search for the best solution. After achieving the fitted regression, the response surface fitting errors  $\varepsilon_\mu$  and  $\varepsilon_\sigma$  were also taken into account as random variables. The best-fit polynomial functions are given by:

$$D_\mu = (\theta_{\mu 1} + \theta_{\mu 2} Li + \theta_{\mu 3} Wi + \theta_{\mu 4} C_y^2 + \theta_{\mu 5} C_y Wi + \theta_{\mu 6} W + \theta_{\mu 7} C_y + \theta_{\mu 8} C_y i) \times (1 - \varepsilon_\mu) \quad (3)$$

$$D_\sigma = (\theta_{\sigma 1} + \theta_{\sigma 2} i + \theta_{\sigma 3} i^4 + \theta_{\sigma 4} C_y Li^2 + \theta_{\sigma 5} W + \theta_{\sigma 6} i^3 + \theta_{\sigma 7} C_y^2) \times (1 - \varepsilon_\sigma) \quad (4)$$

Eq. (3) and Eq. (4) are the polynomial functions with the use of Bayesian inference for the mean and the standard deviation of the maximum interstorey drift, respectively. The goodness-of-fit (square error) of the  $D_\mu$  and  $D_\sigma$  models were found to be 0.99 and 0.97, respectively.

Table 4. Posterior statistics of the Bayesian regression coefficients in the Eq. (3) and Eq. (4).

Eq. (3)	Mean	STDV (%)	Eq. (4)	Mean	STDV (%)
$\theta_{\mu 1}$	0.017342	7.9	$\theta_{\sigma 1}$	0.003511	15.21
$\theta_{\mu 2}$	0.011398	11.44	$\theta_{\sigma 2}$	0.007203	30.18
$\theta_{\mu 3}$	0.006724	2.01	$\theta_{\sigma 3}$	0.000276	17
$\theta_{\mu 4}$	0.288401	21.17	$\theta_{\sigma 4}$	0.003514	9.51
$\theta_{\mu 5}$	0.020175	32.74	$\theta_{\sigma 5}$	-0.00366	30.83
$\theta_{\mu 6}$	-0.00423	25.54	$\theta_{\sigma 6}$	-0.00136	16.24
$\theta_{\mu 7}$	-0.14444	5.8	$\theta_{\sigma 7}$	-0.03454	6.16
$\theta_{\mu 8}$	-0.02216	10.24			

The mean and standard deviation of  $\epsilon_\mu$  were found to be 0.00015 and 0.055, respectively. Similarly, the mean and standard deviation of  $\epsilon_\sigma$  were found to be 0.00033 and 0.089, respectively. The posterior distribution of Eq. (3) and Eq. (4) is shown in Table 4. The posterior correlation coefficients of regression coefficients were also examined to ensure no strong correlation exists. To ensure the accuracy of proposed regression models, diagnostics were performed for each inference. As previously mentioned, the mean error for both the mean and standard deviation of the interstorey drift was sufficiently small relative to the drift values. Moreover, Graphical diagnoses are utilized to evaluate the accuracy of the regression equations. The normal distribution of the model error is confirmed by the Q-Q plot shown in Figure 3, where quantiles of the model residual are plotted against normal theoretical quantiles. Due to the symmetry and alignment of the points along the reference line, it can be observed that the residuals exhibited a normal distribution. The presence of heteroskedasticity, indicated by significant changes in the standard deviation of the model error across the range of variables, is also examined. The residuals plot in Figure 4 shows that the data points were evenly distributed around the center, demonstrating that the model did not show signs of heteroskedasticity. Figure 5 exhibits the median model predictions versus observed data. This plot shows that the model had a fair prediction of the actual data.

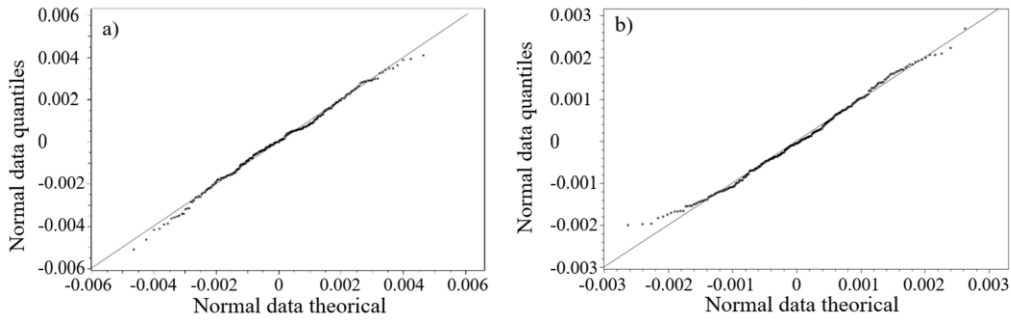


Figure 3. Quantile-Quantile plot: a) Mean of the drifts; b) Standard deviation of interstorey drifts

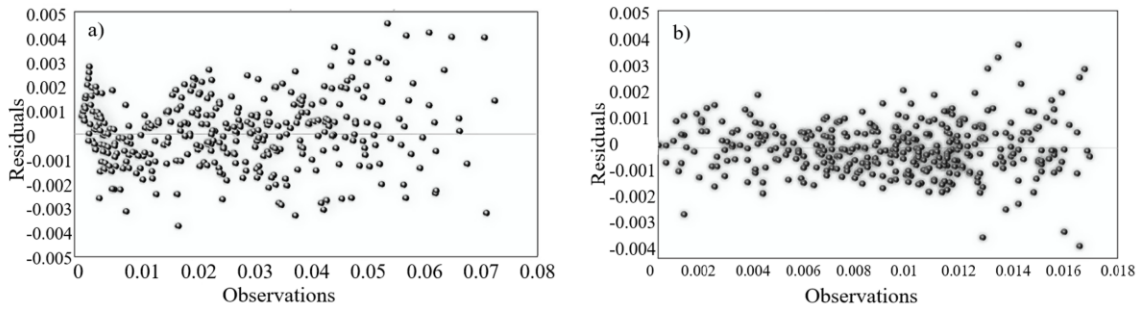


Figure 4. Residual plot: a) Mean of the drifts; b) Standard deviation of drifts

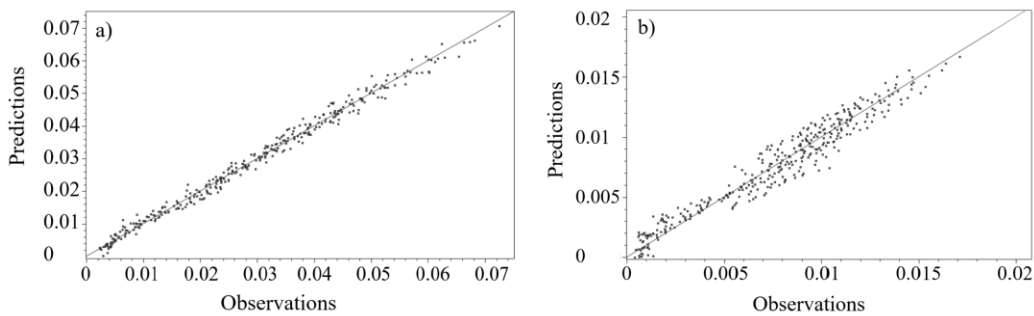


Figure 5. Prediction model a) Mean of the drifts b) Standard deviation of interstorey drifts

### Performance Function and Demand Model

For conducting the reliability analysis of the hybrid timber-steel frame system, the limit-state function is defined as  $g(X)$  and the failure probability is given by:

$$P_f = Prob[g(X) = \delta - D(X) < 0] \quad (5)$$

where the demand model ( $D$ ) was expressed in term of six random variables  $X = \{i, l, w, cy, \varepsilon_\mu, \varepsilon_\sigma\}$  and  $\delta$  was the drift ratio capacity. Record-to-record variability was involved through the mean and standard deviation of the peak interstorey drift. In order to calculate the design point in the reliability analysis, Eq. (5) should be transformed to an explicit function symmetric around the origin. A lognormal cumulative distribution is usually considered for maximum interstorey drift ratio at different performance levels. Eq. (6) describes the closed form solution, which was developed by Li et al [26].

$$D(X) = \frac{D_\mu}{\sqrt{1+v^2}} \exp(R_N \sqrt{Ln(1+v^2)}) \quad (6)$$

Where  $v$  is the coefficient of variation of the peak interstorey drift ( $D_\mu/D_\sigma$ ); and  $R_N$  is the standard normal variate.

### Reliability Method

In order to calculate the failure probability, the Second-order reliability method (SORM) was employed using the explicit function previously described for the limit-state function. The SORM approach approximates the limit-state function with a hyper-paraboloid second-order function. As the demand model is nonlinear with respect to the random variables, SORM enables accurate estimation of the limit-state function.

Reliability sensitivities were obtained by calculating the importance vectors that indicate the relative importance of parameters. One such measures is the alpha-vector ( $\alpha$ ), which represents the negative and normalized version of the limit-state function gradient [12]. The magnitude of Alpha-vector is an appropriate importance measure for random variables in the standard normal space and when variables are uncorrelated. The individual components of the alpha-vector determine the contribution of each parameter to the total variance. The absolute values of alpha's components were compared across the random variables, revealing that ground motion intensity ( $\alpha_i = 0.68$ ) had the greatest impact on failure probability. Among the other three factors the yield base shear coefficient ( $\alpha_{cy} = 0.39$ ), the seismic weight ( $\alpha_w = 0.22$ ) and the length of the RBS connection ( $\alpha_l = 0.17$ ) had the most significant effect, respectively. Another importance measure, Gamma-vector, was introduced by Der Kiureghian [12], which can be utilized to rank the variables in the original space, overcoming the limitations of correlated parameters. The same trend for the importance of random variables was found using the Gamma-vector criteria.

The performance functions were implemented in Rt, a computer program for multi-model reliability and risk analysis [27]. First, the variables in the original space were transformed into the standard normal space to make the random variables uncorrelated. The probability content was then formulated outside a hyper-paraboloid. The joint probability density function has a radial symmetry around the origin. Therefore, the point closest to the origin has the highest failure probability which is known as the design point. NATAF transformation [28] has been used for this purpose. An optimization problem was solved using the iHLRF algorithm [29]. In each step, the convergence direction vector was calculated, and the ARMIJO search rule [30] was adopted to determine the step size.

### FRAGILITY ANALYSIS AND RELIABILITY ANALYSIS RESULTS

The failure probability was determined for three seismic performance levels; the immediate occupancy (1.5% MISD limit), life safety (2.5% MISD limit) and collapse prevention (5% MISD limit). As stated before, four main random variables were considered along with two random variables representing the model errors.

The probability of failure was less than 0.6% for all structures at life safety performance level. Table 5 presents the  $C_y$  values and corresponding reliability indices for the first model designed with  $Rd = 5$ . Similar trends were observed for the other models. The analysis reveals that, with other random variables held constant, an increase in  $C_y$  leads to an increase in the reliability index for the immediate occupancy performance level. However, for the life safety and collapse prevention levels, the increase in the reliability index becomes less significant as  $C_y$  exceeds 0.3. Figure 6 depicts the joint impact of the seismic weight and RBS connection length on the reliability index for the life safety level (MISD = 2.5%). The results reveal that the

models with a larger seismic weight exhibited lower reliability indices. Moreover, an increase in the RBS connection length was found to reduce the reliability index.

Table 5. Reliability index with different  $C_y$  ratios for three performance levels (drift limits) of model No.1.

$C_y$	1.5%	2.5%	5%
0.34	0.665	2.170	4.726
0.32	0.661	2.167	4.725
0.30	0.659	2.162	4.722
0.28	0.652	2.155	4.701
0.26	0.631	2.154	4.666
0.24	0.611	2.115	4.620
0.22	0.592	2.076	4.567
0.20	0.563	2.038	4.514
0.18	0.547	2.001	4.463
0.16	0.532	1.965	4.412
0.14	0.516	1.928	4.362
0.12	0.502	1.893	4.312
0.10	0.484	1.858	4.264

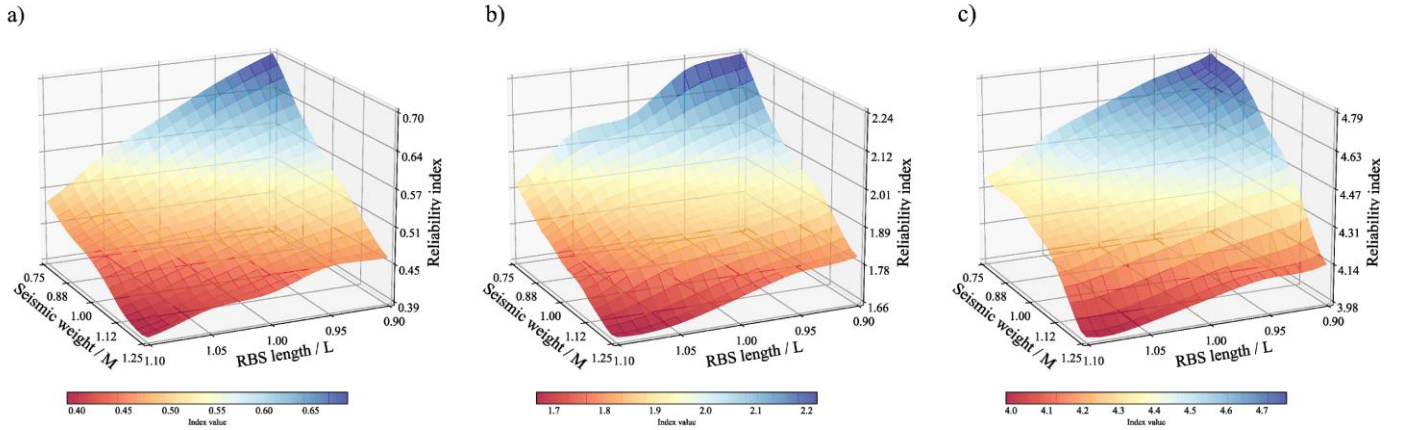


Figure 6. Reliability index for the model No.1 with different seismic weight and RBS length (proportional to the initial weight) : a) Immediate occupancy (1.5% MISD); b) Life safety (2.5% MISD); c) Collapse prevention (5% MISD).

Fragility analysis is important for estimating the risk from potential earthquakes. Herein, the fragility curves were estimated using the Bayesian regression equations and compared to the ones directly from curves. The fragility is defined as the failure probability that the drift demand ( $D$ ) exceeds a specific limit ( $\delta$ ), given a certain spectral acceleration [31]. This can be formulated by equations that are developed by Rahnema and Krawinkler [32] and are presented in Eq. (7). The standard normal integral has been used:

$$P = (D > \delta | S_a = x) = \int \left( \frac{1}{\xi x \sqrt{2\pi}} \exp \left[ -0.5 \left( \frac{\ln(x) - \lambda}{\xi} \right)^2 \right] \right) dx$$

$$\lambda = \ln(D_\mu) - 0.5\xi^2, \text{ and } \xi^2 = \ln \left( 1 + \left( \frac{D_\sigma}{\mu} \right)^2 \right) \quad (7)$$

Where  $\lambda$  and  $\xi$  are the parameters that measure the inherent randomness in seismic capacity, which are determined based on the mean and standard deviation of the demand model estimated using the Bayesian regression method. The fragility curves presented in Figure 7 demonstrate that the results obtained from the Bayesian regression analysis are in excellent agreement with those obtained directly from the IDA database.

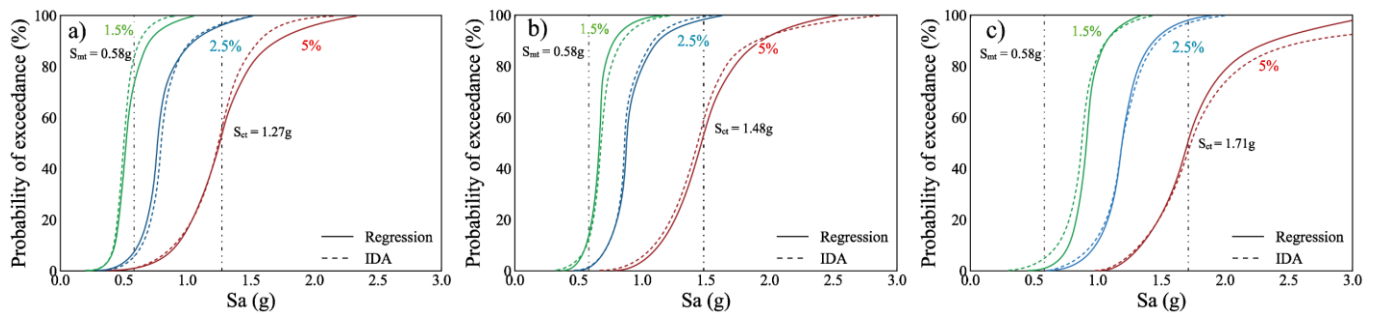


Figure 7. Fragility curves of the immediate occupancy (1.5% MISD), life safety (2.5% MISD) and collapse prevention (5% MISD) based on IDA and regression analysis for reference models: a) Model No.1; b) Model No.2; c) Model No.3.

## CONCLUSION

The objective of this study was to assess the seismic reliability of a novel hybrid timber-steel moment-resisting system using the response surface method obtained through Bayesian regression inference. The study considered four sources of uncertainty in the seismic response: ground motion intensity, seismic weight, RBS connection length, and the yield base shear coefficient, along with the response fitting errors. The results showed that the system was able to withstand high-intensity ground motions and localize damage to the steel links. The following conclusions are drawn from this study:

- It was found that the hybrid steel-timber structure designed with  $R_d = 5$  exhibited a probability of failure of 0.6% at a seismic hazard of 2% probability of exceedance in 50 years. The structure experienced collapse at intensities exceeding two times the design level earthquake, indicating that  $R_d = 5$  is a safe factor for seismic design.
- The study found that the overall rotation of the connection and adjacent elements approached the same value as the interstorey drift value with an increasing intensity of ground motion, which justifies the use of a 5% interstorey drift limit for the collapse point.
- The reliability analysis of the studied hybrid timber-steel moment resisting system revealed that models designed with higher  $C_y$  values exhibited greater reliability index. However, it was observed that increasing the  $C_y$  value beyond 0.3 did not result in a significant change in the reliability index for the life safety and collapse prevention performance levels. This finding suggests that designing stiffer systems with lower  $R_d$  factors, and thus higher  $C_y$  values, may not necessarily enhance seismic safety margins in proportion to the reduction in the  $R_d$  factor. One possible explanation is that stiffer lateral load-resisting systems tend to absorb more energy from ground excitations, resulting in a more severe response at near-collapse states.
- The study also identified the most influential parameters on the reliability of the hybrid timber-steel moment-resisting system, which were found to be the intensity measure,  $C_y$ , seismic weight, and RBS length, in that order. An increase in the design RBS length led to a decrease in the reliability index. Similarly, an increase in seismic weight increased the probability of failure.
- The study also conducted seismic fragility analysis and probabilistic seismic demand analysis for the prototype models of the hybrid timber-steel frames. The Bayesian equations used in this analysis predicted the probability of collapse fairly accurately, compared to the fragility curves obtained directly from IDA analysis. Moreover, the response surface method allowed for the reliability analysis to be done at a lower computational cost. The consistency between the two sets of results provides further validation for the effectiveness and reliability of the Bayesian regression method in estimating the fragility curves of structures. These findings underscore the potential of the Bayesian regression approach as a powerful tool for seismic risk assessment and decision-making in structural engineering.

## REFERENCES

- [1] Abed, J., Rayburg, S., Rodwell, J., and Neave, M. (2022). "A Review of the Performance and Benefits of Mass Timber as an Alternative to Concrete and Steel for Improving the Sustainability of Structures". *Sustainability*, 14(9), 5570.
- [2] National Research Council of Canada. (2020). *National Building Code of Canada (NBCC)*. Canadian Commission on Building and Fire Code, Ottawa, Canada.
- [3] Andreolli, M., Piazza, M., Tomasi, R., and Zandonini, R. (2011). "Ductile moment-resistant steel-timber connections". In *Proceedings of the Institution of Civil Engineers - Structures and Buildings*. 164, 65-78.

- [4] Komatsu, K. et al. (2018). "Development of glulam moment-resisting joint having high initial stiffness, clear yielding moment and rich ductility". In *Proceedings of the 15th World Conference on Timber Engineering*, Seoul, South Korea.
- [5] Komatsu, K., Teng, Q., Li, Z., Zhang, X., and Que, Z. (2019). "Experimental and analytical investigation on the nonlinear behaviors of glulam moment-resisting joints composed of inclined self-tapping screws with steel side plates". *Advances in Structural Engineering*, 22(15), 3190-3206.
- [6] Gilbert, C., Gohlich, R., and Erochko, J. (2015). "Nonlinear dynamic analysis of innovative high R-factor hybrid timber-steel buildings". In *Proceedings of the 11th Canadian Conference on Earthquake Engineering*, Victoria, Canada.
- [7] Montuori, R., and Sagarese, V. (2018). "The use of steel RBS to increase ductility of wooden beams". *Engineering Structures*, 169, 154-161.
- [8] Papadrakakis, M., Tsompanakis, Y., Lagaros, N. D., and Fragiadakis, M. (2004). "Reliability based optimization of steel frames under seismic loading conditions using evolutionary computation". *Journal of Theoretical and Applied Mechanics*, 42, 585-608.
- [9] Khatibinia, M., Fadaee, M. J., Salajegheh, J., and Salajegheh, E. (2013). "Seismic reliability assessment of RC structures including soil-structure interaction using wavelet weighted least squares support vector machine". *Reliability Engineering and System Safety*, 110, 22-33. doi:<https://doi.org/10.1016/J.RESS.2012.09.006>
- [10] Kia, M., and Banazadeh, M. (2016). "Closed-form fragility analysis of the steel moment resisting frames"., *Steel and Composite Structures*, 21, 93-107. doi:<https://doi.org/10.12989/scs.2016.21.1.093>
- [11] Kia, M., Banazadeh, M., and Bayat, M. (2018). "Rapid seismic vulnerability assessment by new regression-based demand and collapse models for steel moment frames". *Earthquake and Structures*, 14, 203-214. doi:<https://doi.org/10.12989/eas.2018.14.3.203>
- [12] Der Kiureghian, A. (2005). *First-and second-order reliability methods*. Engineering Design Reliability Handbook, 14.
- [13] Box, G. E., and Wilson, K. B. (1992). "On the experimental attainment of optimum conditions". *Breakthroughs in statistics: methodology and distribution*, 270-310.
- [14] Gohlich, R., Erochko, J., and Woods, J. E. (2018). "Experimental testing and numerical modelling of a heavy timber moment-resisting frame with ductile steel links". *Earthquake Engineering and Structural Dynamics*. 47. 1460-1477.
- [15] Canadian Standards Association- CSA (2019). *CSA O86: Engineering Design in Wood*. Mississauga, ON. Canada.
- [16] Canadian Standards Association- CSA (2019). *CSA S16: Design of Steel Structures*. Mississauga, ON. Canada.
- [17] McKenna, F., Fenves, G., Scott, H., and Jeremic, B. (2000). *Open System for Earthquake Engineering Simulation (OpenSees)*. [Computer Software]: Pacific Earthquake Engineering Research Center, University of California, Berkeley, CA, USA.
- [18] Menegotto, M. (1973). "Method of analysis for cyclically loaded RC plane frames including changes in geometry and non-elastic behavior of elements under combined normal force and bending". In *Proceedings of IABSE Symposium on Resistance and Ultimate Deformability of Structures Acted on by Well Defined Repeated Loads*.
- [19] Gupta, A., and Krawinkler, H. (1999). *Seismic demands for performance evaluation of steel moment resisting frame structures (SAC Task 5.4. 3)*. John A. Blume Earthquake Engineering Center.
- [20] FEMA P 695. (2009). *Quantification of Building Seismic Performance Factors*. Applied Technology Council. Federal Emergency Management Agency, Washington, USA.
- [21] Halchuk, S., Allen, T. I., Adams, J., and Rogers, G. C. (2014). *Fifth generation seismic hazard model input files as proposed to produce values for the 2015 National Building Code of Canada*. Geological Survey of Canada Open File, 7576(18), 57-123.
- [22] Vamvatsikos, D., and Cornell, A. (2002). "The incremental dynamic analysis and its application to performance-based earthquake engineering". In *Proceedings of the 12th European conference on earthquake engineering*, 40, 1375-92.
- [23] Federal Emergency Management Agency - FEMA (2000). *FEMA P-350: Recommended seismic design criteria for new steel moment-frame buildings*. SAC Joint Venture, Washington, DC, USA.

- [24] National Research Council Canada (NRC), Canadian Construction Material Centre (CCMC). (2021). *Technical guide for evaluation of seismic force resisting systems and their force modification factors for use in the National Building Code of Canada with concepts illustrated using a cantilevered wood CLT shear wall example*.
- [25] Cohen, A. C. (1959). "Simplified Estimators for the Normal Distribution When Samples Are Singly Censored or Truncated". *Technometrics*, 1(3), 217-237.
- [26] Li, M., Lam, F., Foschi, R. O., Nakajima, S., and Nakagawa, T. (2012). "Seismic performance of post-and-beam timber buildings II: reliability evaluations". *Journal of Wood Science*, 58, 135-143. doi:<https://doi.org/10.1007/s10086-011-1232-8>
- [27] Mahsuli, M., and Haukaas, T. (2013). "Computer Program for Multimodel Reliability and Optimization Analysis". *Journal of Computing in Civil Engineering*. 27. 87-98. doi:[https://doi.org/10.1061/\(ASCE\)CP.1943-5487.0000204](https://doi.org/10.1061/(ASCE)CP.1943-5487.0000204).
- [28] Nataf, A. (1962). "Determination des Distribution don t les marges sont Donnees". *Comptes Rendus de l Academie des Sciences*, 225, 42-43.
- [29] Zhang, Y., and Der Kiureghian, A. (1997). *Finite element reliability methods for inelastic structures*. Department of Civil and Environmental Engineering, University of California, CA, USA.
- [30] Keshtegar, B. (2017). "A hybrid conjugate finite-step length method for robust and efficient reliability analysis". *Applied Mathematical Modelling*, 45, 226-237.
- [31] Lu, D., Yu, X., Pan, F., and Wang, G. (2008). "Probabilistic seismic demand analysis considering random system properties by an improved cloud method". In *Proceedings of the 14th World Conference on Earthquake Engineering*, Beijing, China.
- [32] Rahnama, M., and Krawinkler, H. (1993). *Effects of soft soil and hysteresis model on seismic demands (Vol. 108)*. Stanford: John A. Blume Earthquake Engineering Center.